

# Excited-State Characteristics of Tetracyanonitridorhenium(V) and -technetium(V) Complexes with N-Heteroaromatic Ligands

Hayato Ikeda,<sup>†</sup> Akitaka Ito,<sup>‡</sup> Eri Sakuda,<sup>‡,§</sup> Noboru Kitamura,<sup>‡,§</sup> Tsutomu Takayama,<sup>⊥</sup> Tsutomu Sekine,<sup>||</sup> Atsushi Shinohara,<sup>†</sup> and Takashi Yoshimura<sup>\*,#</sup>

<sup>†</sup>Department of Chemistry, Graduate School of Science, Osaka University, Toyonaka 560-0043, Japan

<sup>‡</sup>Department of Chemistry, Faculty of Science, Hokkaido University, Sapporo 060-0810, Japan

<sup>§</sup>Department of Chemical Sciences and Engineering, Graduate School of Chemical Sciences and Engineering, Hokkaido University, Sapporo 060-0810, Japan

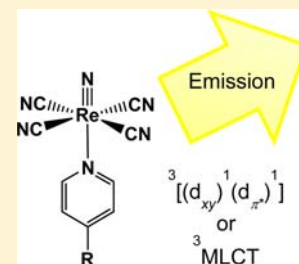
<sup>⊥</sup>Department of Chemistry, Daido University, Nagoya 457-8530, Japan

<sup>||</sup>Center for the Advancement of Higher Education, Tohoku University, Sendai 980-8576, Japan

<sup>#</sup>Radioisotope Research Center, Osaka University, Suita 565-0871, Japan

## Supporting Information

**ABSTRACT:** Six-coordinate tetracyanonitridorhenium(V) and -technetium(V) with axial N-heteroaromatic ligands,  $(\text{PPh}_4)_2[\text{MN}(\text{CN})_4\text{L}]$  [ $\text{M} = \text{Re}$ ,  $\text{L} = 4$ -(dimethylamino)pyridine (dmap), 3,5-lutidine (lut), 4-picoline (pic), 4-phenylpyridine (ppy), pyridine (py), 3-benzoylpyridine (3bzpy), 4,4'-bipyridine (bpy), pyrazine (pz), 4-cyanopyridine (cpy), or 4-benzoylpyridine (4bzpy);  $\text{M} = \text{Tc}$ ,  $\text{L} = \text{dmap}$ , lut, pic, py, pz, or cpy)] were synthesized and characterized. The crystal structures of 11 complexes were determined by single-crystal X-ray analysis. All of the complexes showed photoluminescence in the crystalline phase at room temperature. The emission maximum wavelengths ( $\lambda_{\text{em}}$ ) of the rhenium complexes with dmap, lut, pic, ppy, or py were similar to one another with a quite high emission quantum yield ( $\Phi_{\text{em}}$ ):  $\lambda_{\text{em}} = 539\text{--}545$  nm,  $\Phi_{\text{em}} = 0.39\text{--}0.93$ , and emission lifetime ( $\tau_{\text{em}}$ ) = 10–45  $\mu\text{s}$  at 296 K. The emission spectra at 77 K exhibited vibronic progressions, and the emissive excited state is characterized as  $^3[(d_{xy})^1(d_{\pi^*})^1]$  ( $d_{\pi^*} = d_{xz}, d_{yz}$ ). On the other hand, the emission maximum wavelength of the rhenium complex with 3bzpy, bpy, pz, cpy, or 4bzpy was significantly dependent on the nature of the axial ligand in the crystalline phase:  $\lambda_{\text{em}} = 564\text{--}669$  nm,  $\Phi_{\text{em}} \leq 0.01\text{--}0.36$ , and  $\tau_{\text{em}} = 0.03\text{--}13.3$   $\mu\text{s}$  at 296 K. The emission spectra at 77 K in the crystalline phase did not show vibronic progressions. The emissive excited state of the rhenium complex with bpy, pz, cpy, or 4bzpy is assignable to originate from the metal-to-N-heteroaromatic ligand charge-transfer (MLCT)-type emission with a spin-triplet type. The change in the excited-state characteristics of rhenium complexes by the N-heteroaromatic ligand is a result of stabilization of the  $\pi^*$  orbital of the N-heteroaromatic ligand to a lower energy level than the  $d_{\pi^*}$  orbitals. The emission spectral shapes of technetium complexes were almost independent of the nature of the N-heteroaromatic ligand with  $\lambda_{\text{em}} = 574\text{--}581$  nm at room temperature. The different emission characteristics between the pz and cpy coordinate rhenium complexes and the technetium analogues would be due to stabilization of technetium-centered orbitals compared with the rhenium ones in energy.



## INTRODUCTION

Photoluminescence of metal complexes have attracted much interest for a long time with respect to studies of the excited-state properties, chemical reactions in the excited states, and development of photodevices. The nature of the lowest-energy electronic transition in a metal complex is determined by the combination of a metal ion and a ligand. Control of the excited-state characteristics is still significantly important to realize a desirable compound for a light-driven system. The technetium complexes showing photoluminescence at room temperature are still limited.<sup>1–7</sup> It is recognized that the photoluminescence of  $d^2$  oxo- or nitridomolybdenum(IV),<sup>8,9</sup> -technetium(V),<sup>1,6,7</sup> -rhenium(V),<sup>1,6,7,10–28</sup> and -osmium(VI)<sup>22,29–41</sup> complexes arises from their  $^3[(d_{xy})^1(d_{\pi^*})^1]$  ( $d_{\pi^*} = d_{xz}, d_{yz}$ ) excited states. In the case of photoemissive dioxo- and nitridorhenium(V) and -technetium(V) complexes, a number of neutral or anionic ligands such as diphosphine, N-heteroaromatic, and cyanido ligands

have been introduced to the equatorial positions of the metal ions.<sup>1,6,7,10–12,14–28</sup> The emission maximum wavelengths ( $\lambda_{\text{em}}$ ) of the rhenium and technetium complexes in the solid state or solution depend on the nature of the equatorial and axial ligands. In practice, the  $\lambda_{\text{em}}$  values of the complexes at room temperature range from ca. 500 to 1000 nm, with the emission lifetimes ( $\tau_{\text{em}}$ ) being several dozens of nanoseconds to several hundreds of microseconds.<sup>1,6,7,10–12,14–28</sup> The emission quantum yields ( $\Phi_{\text{em}}$ ) of the  $d^2$  oxo- or nitridometal complexes in solution at room temperature have also been reported to be  $<10^{-5}\text{--}0.04$ .<sup>11,14,15,18,19,40</sup> Previously, we reported the photoluminescent properties of six-coordinate  $[\text{MN}(\text{CN})_4\text{L}]^{2-}$  ( $\text{M} = \text{Re}$ ,  $\text{L} = \text{methanol}$ , ethanol, acetone, or acetonitrile;  $\text{M} = \text{Tc}$ ,  $\text{L} = \text{methanol}$ ) and five-coordinate  $[\text{MN}(\text{CN})_4]^{2-}$  complexes ( $\text{M} = \text{Re}$  and  $\text{Tc}$ ).<sup>7</sup>

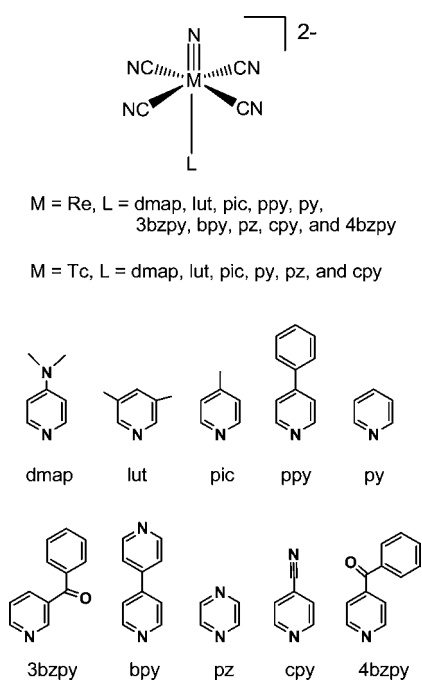
Received: November 10, 2012

Published: May 16, 2013

The photoluminescence of the five-coordinate rhenium(V) and technetium(V) complexes was relatively weak compared with that of the relevant six-coordinate complex. Furthermore, the  $\lambda_{\text{em}}$ ,  $\Phi_{\text{em}}$ , and  $\tau_{\text{em}}$  values of the six-coordinate complexes in the solid state at 296 K were strongly dependent on the nature of the coordinate solvent ligand:  $\lambda_{\text{em}} = 527\text{--}548\text{ nm}$ ,  $\Phi_{\text{em}} \leq 0.01\text{--}0.34$ , and  $\tau_{\text{em}} = 0.41\text{--}21\text{ }\mu\text{s}$ . In these complexes, we demonstrated that the photoluminescence from the complex could be switched reversibly by interconversion reactions between the six- and five-coordinate complexes as well as between the six-coordinate complexes in the solid phase.

In the present study, we introduced various N-heteroaromatic ligands to the trans positions of the nitrido ligands in tetracyanonitridorhenium(V) and -technetium(V) complexes, as shown in Chart 1, and studied the emission properties of

Chart 1



$[\text{ReN}(\text{CN})_4\text{L}]^{2-}$ , where L was 4-(dimethylamino)pyridine (dmap), 3,5-lutidine (lut), 4-picoline (pic), pyridine (py), 4-phenylpyridine (ppy), 3-benzoylpyridine (3bzpy), 4,4'-bipyridine (bpy), pyrazine (pz), 4-cyanopyridine (cpy), or 4-benzoylpyridine (4bzpy). The photoluminescence of the  $[\text{TcN}(\text{CN})_4\text{L}]^{2-}$  complexes with dmap, lut, pic, py, pz, or cpy was also investigated. We found that the  $\Phi_{\text{em}}$  value of the py coordinate rhenium complex was as high as 0.93 and remarkably high compared with the reported  $d^2$  dioxo- and nitridometal complexes. The rhenium complexes showed two types of emission characteristics. One is emission from the  $^3[(d_{xy})^1(d_{\pi^*})^1]$  excited state (L = dmap, lut, pic, py, or ppy) with contribution of the nitrido ligand, showing very similar  $\lambda_{\text{em}}$  (539–545 nm), quite high  $\Phi_{\text{em}}$  (0.39–0.93), and long emission lifetime ( $\tau_{\text{em}} = 10\text{--}45\text{ }\mu\text{s}$ ) at 296 K. The other is the spin-triplet metal-to-N-heteroaromatic ligand charge-transfer ( $^3\text{MLCT}$ ) emission for  $[\text{ReN}(\text{CN})_4\text{L}]^{2-}$  (L = bpy, pz, cpy, or 4bzpy), demonstrating large variations of the emission properties of the complex by the nature of the N-heteroaromatic ligand:  $\lambda_{\text{em}} = 578\text{--}669\text{ nm}$ ,  $\Phi_{\text{em}} \leq 0.01\text{--}0.18$ , and  $\tau_{\text{em}} = 0.03\text{--}9.7\text{ }\mu\text{s}$  at 296 K. The results are discussed on the basis of the energy-gap dependence of the nonradiative decay rate constant for the complex having the MLCT excited

state. The emission maximum wavelengths of the technetium complexes were almost independent of the nature of the N-heteroaromatic ligand. On the basis of these new findings, we demonstrate that the low-energy-lying  $\pi^*$  orbital of an N-heteroaromatic ligand and the energies of the d orbitals determine primarily the nature of the emissive excited state of a  $d^2$  nitridometal complex.

## EXPERIMENTAL SECTION

**Materials.** All commercially available reagents were used as received. The isotope  $^{99}\text{Tc}$  was used to synthesize all of the technetium complexes reported in this paper. **Caution!**  $^{99}\text{Tc}$  is a low-energy  $\beta^-$  emitter ( $E_{\text{max}} = 290\text{ keV}$ ) with a half-life of  $2.11 \times 10^5$  years.  $(\text{PPh}_4)_2[\text{ReN}(\text{CN})_4]$  and  $(\text{PPh}_4)_2[\text{TcN}(\text{CN})_4]$  were prepared according to the literature.

**Preparation of the Complexes.** The new complexes were synthesized by similar methods. The detailed experimental procedures are described in the Supporting Information. The preparation of **Re-dmap** is described as an example.  $(\text{PPh}_4)_2[\text{ReN}(\text{CN})_4]$  (39.5 mg, 0.0402 mmol) and dmap (169.5 mg, 1.387 mmol) were dissolved in 3 mL of acetonitrile, and then 7 mL of diethyl ether was layered on the solution. The solution was left for several days to form yellow crystals. The crystals collected were washed with diethyl ether and left for 1 h in vacuo. **Re-ppy**, **Re-bpy**, and **Tc-dmap** were also obtained from acetonitrile/diethyl ether. **Re-lut**, **Re-pic**, **Re-3bzpy**, **Re-cpy**, **Re-4bzpy**, **Tc-lut**, **Tc-pic**, **Tc-pz**, and **Tc-cpy** were afforded from dichloromethane/diethyl ether. **Re-py** and **Tc-py** were obtained from pyridine/diethyl ether. Yields: **Re-dmap**, 86.6%; **Re-lut**, 92.5%; **Re-pic**, 42.1%; **Re-ppy**, 79.8%; **Re-py**, 95.8%; **Re-3bzpy**, 87.5%; **Re-bpy**, 73.0%; **Re-pz**, 74.1%; **Re-cpy**, 52.7%; **Re-4bzpy**, 87.7%; **Tc-dmap**, 73.1%; **Tc-lut**, 38.6%; **Tc-pic**, 45.1%; **Tc-py**, 94.7%; **Tc-pz**, 97.6%; **Tc-cpy**, 80.6%.

**X-ray Crystallography.** The single-crystal X-ray data were collected at  $-103\text{ }^\circ\text{C}$  on a Rigaku RAXIS diffractometer with graphite-monochromated  $\text{Mo K}\alpha$  radiation. The crystal structures were solved by the Patterson method (*DIRDIF94* or *DIRDIF99*) or direct methods (*SIR 92* or *SIR 2004*). Atomic coordinates and thermal parameters of non-hydrogen atoms were calculated by a full-matrix least-squares method. Calculations were performed using a *TEXSAN* or *Crystal Structure* software package.<sup>42,43</sup> The molecular structures of complex anions were drawn by *ORTEP3*.<sup>44</sup> Crystal data are listed in the Supporting Information, Tables S1 and S2.

**Physical Measurements.**  $^1\text{H}$  NMR spectra were recorded on a Varian Mercury 300 MHz spectrometer. All peaks were referred to the proton signal of  $\text{Si}(\text{CH}_3)_4$  at  $\delta$  0.00. Solid-state diffuse-reflectance UV–vis spectra were measured by a Jasco V-550 spectrophotometer equipped with an integration sphere, and a sample was placed between two silica glass plates. IR spectra were recorded on a Jasco FTIR-4100 spectrophotometer. Elemental analysis was performed by the Analysis Center at Osaka University. For emission lifetime measurements, a sample solid was placed between two nonfluorescent glass plates. A pulsed  $\text{Nd}^{3+}$ :YAG laser (Lotis TII Ltd. LS-2137; 355 nm, fwhm  $\sim 6$  ns) was used as an excitation light source. The emission lifetime was measured by using a streak camera (Hamamatsu Photonics C4334). A liquid-nitrogen cryostat (Oxford Instruments DN1704 optical Dewar and 3120 temperature controller) was used to control the sample temperature. Corrected emission spectra of the rhenium complexes were measured using a multichannel photodetector (Hamamatsu Photonics PMA-11; excitation wavelength = 355 nm). The emission quantum yields were measured by an absolute emission quantum yield measurement system (Hamamatsu Photonics C9920-02) composed of an integrating sphere, a multichannel photodetector (Hamamatsu Photonics PMA-12), and a xenon lamp as an excitation light source (excitation wavelength = 400 nm). For the technetium complexes, corrected emission spectra were recorded on a multichannel photodetector (Hamamatsu Photonics PMA-11), with the excitation wavelength being set at 365 nm ( $\pm 5$  nm) using the combination of a 100 W mercury–xenon lamp (Hoya-Schott HLS 100UM) and an optical filter (Asahi Spectra).

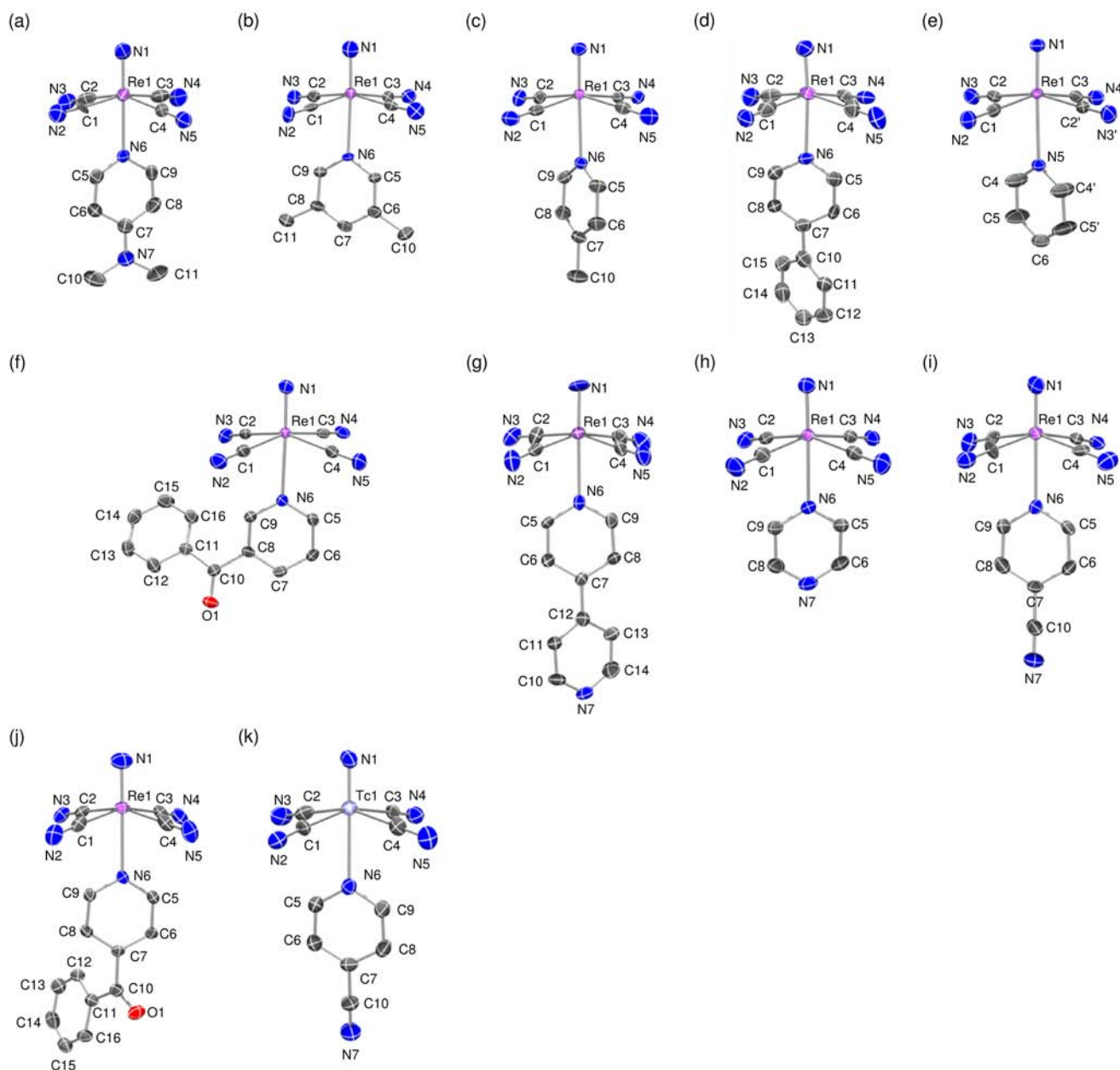


**Figure 1.** ORTEP drawings of the complex anions for **Re-dmap** (a), **Re-lut** (b), **Re-pic** (c), **Re-ppy** (d), **Re-py** (e), **Re-3bzipy** (f), **Re-bpy** (g), **Re-pz** (h), **Re-cpy** (i), **Re-4bzipy** (j), and **Tc-cpy** (k). Hydrogen atoms are omitted for clarity. Thermal ellipsoids are shown at the 50% probability level.

## RESULTS AND DISCUSSION

**Synthesis and Characterization of the Complexes.** The tetracyanonitridorhenium(V) and -technetium(V) complexes with N-heteroaromatic ligands were prepared by the reactions of five-coordinate  $(\text{PPh}_4)_2[\text{MN}(\text{CN})_4]$  ( $M = \text{Re}$  and  $\text{Tc}$ ) with an excess amount of the relevant N-heteroaromatic ligand. In the IR spectra, the absorption bands ascribed to an N-heteroaromatic ligand in  $[\text{MN}(\text{CN})_4\text{L}]^{2-}$  were observed together with those of the  $(\text{PPh}_4)^+$  and  $[\text{MN}(\text{CN})_4]^{2-}$  units, as shown in the Supporting Information, Figures S1–S16. For **Re-py** as an example, the IR absorption bands originating from py were observed at  $1594$  and  $1151\text{ cm}^{-1}$  for  $\nu_{\text{ring(py)}}$  and at  $1135$  and  $1064\text{ cm}^{-1}$  for  $\delta_{\text{C-H(py)}}$ . Similar IR bands ascribed to py were also confirmed for the py coordinate technetium complex, and the IR spectral patterns of the technetium complexes were

very similar to those of the relevant rhenium complexes. The lowest-energy UV–vis reflectance bands and emission spectral bands of the new six-coordinate rhenium and technetium complexes shifted to longer wavelength compared with those of the relevant five-coordinate complexes (vide infra). The 10 rhenium complexes and **Tc-cpy** have been characterized by single-crystal X-ray structure analysis, and the results are reported in the following section.

**Crystal Structures.** The crystal structures of 11 complexes, **Re-dmap**, **Re-lut**, **Re-pic**, **Re-ppy**, **Re-py**, **Re-3bzipy**, **Re-bpy**, **Re-pz**, **Re-cpy**, **Re-4bzipy**, and **Tc-cpy**, were determined. The structures and selected bond distances/angles of these new complexes are summarized in Figure 1 and Table 1, respectively. The complex anions have a distorted octahedral structure, with one nitrido atom being located at the axial site and an N-heteroaromatic ligand being occupied at the trans site

Table 1. Selected Bond Distances (Å) and Angles (deg) of the Tetracyanonitridorhenium(V) and -technetium(V) Complexes

	Re-dmap	Re-lut	Re-pic	Re-ppy	Re-py	Re-3bzpy	Re-bpy	Re-pz	Re-cpy	Re-4bzpy	Tc-cpy
M≡N	1.67(1)	1.73(2)	1.663(3)	1.689(12)	1.657(4)	1.656(5)	1.667(6)	1.662(3), 1.663(3)	1.645(5)	1.638(7)	1.598(5)
M–C	2.09(1)– 2.11(2)	2.109(8)– 2.133(7)	2.110(3)– 2.119(3)	2.070(12)– 2.137(13)	2.103(4)– 2.117(3)	2.112(4)– 2.117(4)	2.106(7)– 2.116(8)	2.104(3)– 2.122(3)	2.092(5)– 2.113(5)	2.101(6)– 2.123(7)	2.113(5)– 2.131(4)
M–N	2.45(1)	2.530(9)	2.5610(19)	2.539(10)	2.560(4)	2.522(4)	2.503(5)	2.525(3), 2.536(3)	2.589(5)	2.531(5)	2.626(4)
N≡M–C	97.5(6)– 100.8(5)	97.6(4)– 99.2(5)	97.54(10)– 99.33(10)	94.1(6)– 104.1(6)	97.41(8)– 100.50(17)	98.13(18)– 100.81(17)	97.7(3)– 100.6(3)	99.27(12)– 100.68(14)	99.8(2)– 100.6(2)	99.1(3)– 101.2(3)	99.66(19)– 100.92(19)
N≡M–N	178.2(5)	177.6(4)	177.53(9)	174.1(5)	177.57(17)	178.52(9)	178.3(3)	178.18(11), 178.81(10)	179.21(16)	178.7(3)	179.01(14)

of the nitrido ligand. The four cyanido ions coordinate at the equatorial positions with M–C bond distances of 2.070(12)–2.137(13) Å and N(nitrido)≡M–C angles of 94.1(16)–104.1(6)° (M = Re and Tc). The bond distance of M≡N(nitrido) is in the range 1.598(5)–1.73(2) Å. The M–C and M≡N(nitrido) bond distances are similar to those of the previously reported tetracyanonitridorhenium(V) and -technetium(V) complexes.<sup>7,45–47</sup> The N(nitrido)≡M–N(arene) angles are 174.1(5)–179.21(16)°, almost linear. The Re–N(arene) bond distances are in the range 2.45(1)–2.626(4) Å, which is significantly long because of the trans influence of the nitrido ligand. The M–N(arene) distance decreases roughly with an increase in the pK<sub>a</sub> value of the free ligand, as shown in the Supporting Information, Figure S17. The shortest and longest Re–N(arene) distances were observed for the dmap (pK<sub>a</sub> of dmap = 9.7) and cpy complexes (pK<sub>a</sub> of cpy = 1.9), respectively.<sup>48</sup> Therefore, the σ-electron-donating ability of an N-heteroaromatic ligand moderately influences the Re–N(arene) bond distance. However, the molecular packing structures of the complexes will also be important for determining the Re–N(arene) bond distances because the Re–N(arene) distances of **Re-lut** [2.530(9) Å] and **Re-pz** [2.525(3) and 2.536(3) Å] are similar to each other, despite the fact that the pK<sub>a</sub> values of lut (6.09) and pz (0.65) are significantly different.<sup>48</sup> In the cpy coordinate technetium complex, the Tc≡N(nitrido) and Tc–N(cpy) bond distances are shorter and longer, respectively, than the relevant values of the rhenium analogue. This trend is also found in the [MN(CN)<sub>4</sub>L]<sup>2–</sup> complexes (M = Re and Tc; L = H<sub>2</sub>O and CH<sub>3</sub>OH).<sup>7,45–47</sup>

**UV–Vis Reflectance Spectroscopy.** The UV–vis reflectance spectra of the rhenium and technetium complexes in the solid phases were studied at room temperature; the spectra are shown in the Supporting Information, Figures S18–S20. It was reported that the UV–vis reflectance spectra of the five-coordinate (PPh<sub>4</sub>)<sub>2</sub>[ReN(CN)<sub>4</sub>] and (PPh<sub>4</sub>)<sub>2</sub>[TcN(CN)<sub>4</sub>] in the solid state showed bands at around 383 and 400 nm, respectively.<sup>7</sup> The six-coordinate CH<sub>3</sub>OH complexes of (PPh<sub>4</sub>)<sub>2</sub>[MN(CN)<sub>4</sub>(CH<sub>3</sub>OH)] (M = Re and Tc) exhibited a maximum wavelength at 387 nm for M = Re and at 408 nm for M = Tc in the solid state.<sup>7</sup> These bands are assigned to a (d<sub>xy</sub>)<sup>2</sup> → (d<sub>xy</sub>)<sup>1</sup>(d<sub>π\*</sub>)<sup>1</sup> transition with d<sub>π</sub>–p<sub>π</sub>(N) overlap, which is best characterized by an electronic transition between the highest occupied molecular orbital (HOMO) and lowest unoccupied molecular orbital (LUMO) in a d<sup>2</sup> nitridorhenium(V) or -technetium(V) complex.<sup>7,17–19,23</sup> In the case of [MnN(CN)<sub>4</sub>]<sup>2–</sup> and [MnN(CN)<sub>5</sub>]<sup>3–</sup>, the electronic absorption transition assigned to (d<sub>xy</sub>)<sup>2</sup> → (d<sub>xy</sub>)<sup>1</sup>(d<sub>π\*</sub>)<sup>1</sup> in the six-coordinate [MnN(CN)<sub>5</sub>]<sup>3–</sup> appears in a longer wavelength than that in the five-coordinate [MnN(CN)<sub>4</sub>]<sup>2–</sup> because the axial CN<sup>–</sup> ligand acts as a π acceptor, and this gives rise to elongation of the Mn≡N distance in the six-coordinate complex due to stabilization of the d<sub>π\*</sub> energy level.<sup>49,50</sup>

The present complexes, **Re-dmap**, **Re-lut**, **Re-pic**, **Re-ppy**, and **Re-py**, exhibited a band maximum (λ<sub>max</sub>) at 414–417 nm in the crystalline phase at 296 K. For simplicity, we classify these complexes as group A. The λ<sub>max</sub> values in group A complexes are almost independent of the kind of N-heteroaromatic ligand. In the case of the technetium complexes, the UV–vis reflectance spectral band features were very similar. The λ<sub>max</sub> values observed for the technetium complexes (413–421 nm) were similar to those of the rhenium analogues in group A. The longer-wavelength shift of the λ<sub>max</sub> value of the

**Table 2. Spectroscopic and Photophysical Data of the Tetracyanonitridorhenium(V) and -technetium(V) Complexes in the Crystalline Phase at 296 and 77 K**

	296 K					77 K	
	$\lambda_{em}/nm$	$\Phi_{em}$	$\tau_{em}/\mu s$ (% component)	$k_r/10^4 s^{-1}$	$k_{nr}/10^4 s^{-1}$	$\lambda_{em}/nm$	$\tau_{em}/\mu s$ (% component)
Re-dmap	539	0.79	36 (70), 10 (30)	2.8	0.74	509, 535, 557	75 (100)
Re-lut	544	0.39	26 (100)	1.5	2.3	514, 540, 565	111 (100)
Re-pic	544	0.79	44 (100)	1.8	0.47	518, 547, 579, 616	142 (100)
Re-ppy	545	0.71	40 (100)	1.8	0.73	525, 551	106 (100)
Re-py	539	0.93	45 (100)	2.1	0.16	513, 539, 569, 604	100 (100)
Re-3bzpy	564	0.36	13.3 (100)	2.7	4.8	555	63.8 (100)
Re-bpy	578	0.18	9.7 (59), 2.5 (41)	2.7	12	572	68 (62), 31(38)
Re-pz	623	0.05	2.7 (19), 0.80 (81)	4	81	597	53 (77), 25 (23)
Re-cpy	649	0.01	0.65 (26), 0.12 (74)	4	400	616	5.0 (3), 1.2 (97)
Re-4bzpy	669	<0.01	0.20 (5), 0.03 (95)		2600 <sup>a</sup>	612	4.2 (12), 0.95 (88)
Tc-dmap	574						
Tc-lut	576						
Tc-pic	580						
Tc-py	576						
Tc-pz	581						
Tc-cpy	580						

<sup>a</sup>The  $k_{nr}$  value was calculated from  $1/\tau_{em}$ .

six-coordinate rhenium and technetium complexes compared with that of the relevant five-coordinate complexes is the same trend as that shown between  $[Mn(CN)_4(CH_3OH)]^{2-}$  and  $[Mn(CN)_4]^{2-}$  (M = Re and Tc) and between  $[MnN(CN)_5]^{3-}$  and  $[MnN(CN)_4]^{2-}$ . Therefore, the band observed at around 420 nm for the six-coordinate rhenium complexes in group A and all of the technetium complexes can be ascribed to the  $(d_{xy})^2 \rightarrow (d_{xy})^1(d_{\pi^*})^1$  transitions with  $d_{\pi}-p_{\pi}(N)$  overlap.

In marked contrast to the group A complexes, the UV-vis reflectance spectral features of **Re-bpy**, **Re-pz**, **Re-cpy**, and **Re-4bzpy** are different from those of the group A complexes: classified as group B. In the group B complexes, the spectra exhibited a shoulder band at around 475 nm. The wavelength of the shoulder band is significantly long compared with the wavelength of  $(d_{xy})^2 \rightarrow (d_{xy})^1(d_{\pi^*})^1$  in the group A complexes. In the case of group A, the edge of the band at the lower-energy side appeared at around 520 nm, while the spectra of the group B complexes extended to longer wavelength (>550 nm), as seen in Figures S18 and S19 in the Supporting Information. These results suggest that the band at around 475 nm in the group B complexes is characterized by the contribution of a longer-wavelength transition band that is different from the one in the  $(d_{xy})^2 \rightarrow (d_{xy})^1(d_{\pi^*})^1$  transition. The edge of the band in the group B complexes shifts to longer wavelength in the sequence of **Re-bpy** < **Re-pz** < **Re-cpy**  $\approx$  **Re-4bzpy**. The sequence observed in the UV-vis reflectance spectra is almost the same as that of the emission maximum wavelength ( $\lambda_{em}$ ) of the complexes (vide infra). We assigned the substantially allowed lowest-energy transition band as the metal-to-N-heteroaromatic ligand charge-transfer (MLCT) transition (vide infra).

In the case of **Re-3bzpy**, the feature of the UV-vis reflectance spectrum was similar to that of the group A complexes. On the other hand, the  $\lambda_{em}$  value shifted to longer wavelength compared with the values in the group A complexes, which is the tendency observed in the group B complexes as described later.

**Emission Spectroscopic and Photophysical Properties.** All of the complexes showed photoluminescence in the crystalline phases at room temperature. Table 2 summarizes the spectroscopic and photophysical data observed in the solid state at 296 and 77 K. Figures 2 and 3 show the emission spectra of

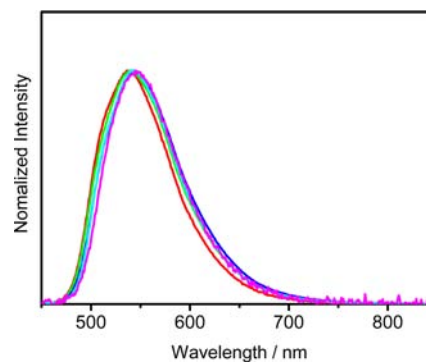


**Figure 2.** Emission spectra of **Re-dmap** (lime green), **Re-lut** (blue), **Re-pic** (cyan), **Re-ppy** (magenta), and **Re-py** (red) at 296 K in the crystalline phase.

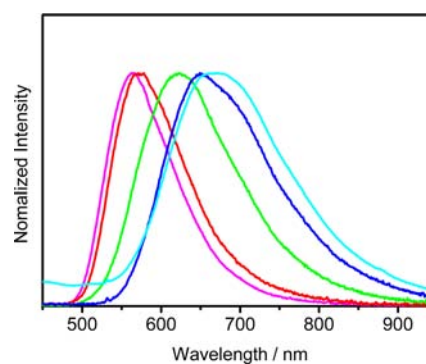


**Figure 3.** Emission spectra of **Re-3bzpy** (magenta), **Re-bpy** (red), **Re-pz** (lime green), **Re-cpy** (blue), and **Re-4bzpy** (cyan) at 296 K in the crystalline phase.

the rhenium complexes in groups A and B and **Re-3bzpy**, respectively, in the crystalline phases at 296 K. The group A complexes in the crystalline phases at 296 K exhibited intense emission with  $\lambda_{em} = 539\text{--}545$  nm,  $\Phi_{em} = 0.39\text{--}0.93$ , and  $\tau_{em} = 10\text{--}45$   $\mu s$ . The spectroscopic and photophysical data of the group B complexes ( $\lambda_{em} = 578\text{--}669$  nm,  $\Phi_{em} \leq 0.01\text{--}0.18$ , and

$\tau_{em} = 0.03\text{--}9.7 \mu\text{s}$ ) are significantly different from those of the group A complexes. The spectroscopic and photophysical data of the group B complexes are characterized by the longer  $\lambda_{em}$ , significantly smaller  $\Phi_{em}$ , and shorter  $\tau_{em}$  than the relevant values of the group A complexes. For **Re-3bzpy**, the  $\lambda_{em}$  value (564 nm) is longer than those of the group A complexes. The  $\lambda_{em}$  values of the group B and **Re-3bzpy** complexes shifted to longer wavelength in the sequence of **Re-3bzpy** (564 nm) < **Re-bpy** (578 nm) < **Re-pz** (623 nm) < **Re-cpy** (649 nm) < **Re-4bzpy** (669 nm). The  $\Phi_{em}$  and  $\tau_{em}$  values of the group B complexes and **Re-3bzpy** are larger and longer in the order of **Re-3bzpy** > **Re-bpy** > **Re-pz** > **Re-cpy** > **Re-4bzpy**.

The emission spectra of the rhenium complexes in groups A and B and **Re-3bzpy** in the crystalline phases at 77 K are shown in Figures 4 and 5, respectively. The group A complexes at 77 K

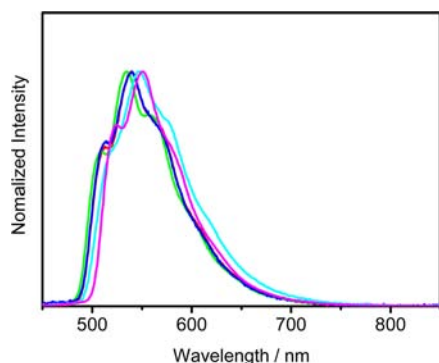


**Figure 4.** Emission spectra of **Re-dmap** (lime green), **Re-lut** (blue), **Re-pic** (cyan), **Re-ppy** (magenta), and **Re-py** (red) at 77 K in the crystalline phase.

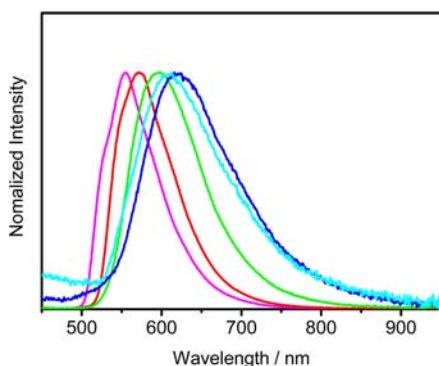


**Figure 5.** Emission spectra of **Re-3bzpy** (magenta), **Re-bpy** (red), **Re-pz** (lime green), **Re-cpy** (blue), and **Re-4bzpy** (cyan) at 77 K in the crystalline phase.

exhibited vibronic structures with progressions of ca.  $1000 \text{ cm}^{-1}$ , and the emission lifetimes were longer ( $75\text{--}142 \mu\text{s}$ ) than the relevant values at 296 K ( $10\text{--}45 \mu\text{s}$ ). The vibrational progressions observed for the complexes are typical for the emission spectra of  $d^2$  nitridometal complexes in the  $^3[(d_{xy})^1(d_{\pi^*})^1]$  excited states.<sup>14,15,25,36,37</sup> The group B and **Re-3bzpy** complexes exhibited large differences in the spectroscopic and photophysical characteristics from the group A complexes for the low-temperature emission spectra in the solid phase. The group B and **Re-3bzpy** complexes showed no vibronic structure in the emission spectra at 77 K. At both 296 and 77 K, the  $\tau_{em}$  values of the group B and **Re-3bzpy** complexes were smaller than those of the group A complexes.

The  $\lambda_{em}$  value of the group B and **Re-3bzpy** complexes shifted to longer wavelength in the sequence of **Re-3bzpy** (555 nm) < **Re-bpy** (572 nm) < **Re-pz** (597 nm) < **Re-4bzpy** (612 nm)  $\approx$  **Re-cpy** (616 nm).

The emission spectra of the technetium complexes in the crystalline phases at 296 K are shown in Figure 6. All of the

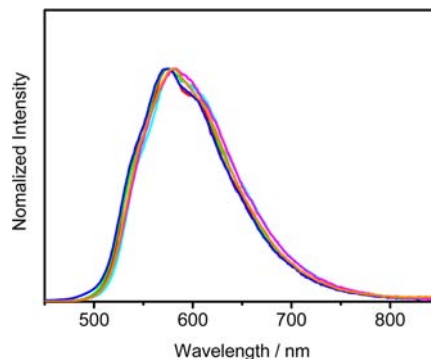


**Figure 6.** Emission spectra of **Tc-dmap** (lime green), **Tc-lut** (blue), **Tc-pic** (cyan), **Tc-py** (red), **Tc-pz** (magenta), and **Tc-cpy** (orange) at 296 K in the crystalline phase.

technetium complexes showed photoluminescence and the maximum wavelengths (574–581 nm) were very similar to one another for all of the technetium complexes studied. This is in marked contrast to the two different emission characteristics between the rhenium group A and B complexes. The emission spectra of the technetium complexes showed vibronic structures. The vibrational progressions (ca.  $1000 \text{ cm}^{-1}$ ) agreed with the  $\nu_{Tc\equiv N}$  stretching band frequency commonly observed for a nitridotechnetium(V) complex.<sup>45,51–58</sup> The spectroscopic features of the technetium complexes were very similar to those of the rhenium group A complexes, although detailed photophysical data ( $\Phi_{em}$  and  $\tau_{em}$ ) of the technetium complexes have not been obtained in the present stage of the investigation. The  $\lambda_{em}$  value for the technetium complex is longer than that for the relevant rhenium complex. The longer wavelength shift of  $\lambda_{em}$  in the technetium complex than that in the relevant rhenium complex has been observed for the methanol coordinate nitridorhenium(V) and -technetium(V) complexes [ $\lambda_{em}$  of  $(PPh_4)_2[M(CN)_4(CH_3OH)]$  in the crystalline phases at room temperature: 559 nm ( $M = Tc$ ) and 527 nm ( $M = Re$ )]. The excited states for the technetium complexes can be assigned to the  $^3[(d_{xy})^1(d_{\pi^*})^1]$  electron configuration.

**Excited-State Characteristics of Nitridotetracyanido-rhenium(V) and -technetium(V) Complexes with N-Heteroaromatic Ligands.** The rhenium complexes classified in the group A and all of the technetium complexes studied possess the  $^3[(d_{xy})^1(d_{\pi^*})^1]$  excited states. The excited-state characteristics are similar to those of the previously reported  $d^2$  nitridometal complexes.<sup>14–19,25,32,33,36,37,39,41</sup> It is worth emphasizing that **Re-py** showed a quite high  $\Phi_{em}$  value of 0.93 among photoluminescent  $d^2$  oxo- and nitridometal complexes whose  $\Phi_{em}$  values are  $<10^{-5}\text{--}0.34$ .<sup>7,11,14,15,18,19,40</sup> The  $\lambda_{em}$  values of the rhenium complexes in group A are similar to one another, although the Re–N(aromatic) bond distance is different, as mentioned before: Re–N = 2.45(1)–2.5610(19) Å for **Re-dmap**, **Re-lut**, **Re-pic**, **Re-ppy**, and **Re-py**. This suggests that the N-heteroaromatic ligand does not play an important role in the orbitals responsible for the emissive excited state:  $d_{xy}$  and  $d_{\pi^*}$  orbitals. The N-heteroaromatic ligands in these complexes influence more or less

the nonradiative decay path(s) from the emissive excited states. It is recognized that thermal deactivation of the emissive excited state through an upper-lying, nonemissive d–d state(s) is one of the factors governing the photoluminescence efficiency.<sup>59</sup> Therefore, the unoccupied  $d_{x^2-y^2}$  and  $d_{z^2}$  orbitals might be destabilized in energy by coordination of an N-heteroaromatic ligand at the axial position, although it is not clear about the nonradiative decay path(s) of the complex in the present stage of the investigation.

The  $\lambda_{em}$ ,  $\Phi_{em}$ , and  $\tau_{em}$  values of the group B complexes were significantly dependent on the nature of the N-heteroaromatic ligand. The spectroscopic and photophysical properties of the group B complexes clearly indicate that the emissive excited state is not the  $^3[(d_{xy})^1(d_{\pi^*})^1]$  excited state. The emission energy values ( $\nu_{em}$ ) of the group B and **Re-3bzipy** complexes are 17700  $\text{cm}^{-1}$  for **Re-3bzipy**, 17300  $\text{cm}^{-1}$  for **Re-bpy**, 16100  $\text{cm}^{-1}$  for **Re-pz**, 15400  $\text{cm}^{-1}$  for **Re-cpy**, and 15000  $\text{cm}^{-1}$  for **Re-4bzipy**. The differences of the emission energy values are similar to the emission energy differences in  $[\text{ReCl}(\text{CO})_3\text{L}_2]$  ( $\text{L} = 3\text{bzipy}$ , **bpy**, or **4bzipy**) showing the MLCT excited state in benzene at 298 K (18300  $\text{cm}^{-1}$  for  $\text{L} = 3\text{bzipy}$ , 17750  $\text{cm}^{-1}$  for  $\text{L} = \text{bpy}$ , and 16700  $\text{cm}^{-1}$  for  $\text{L} = 4\text{bzipy}$ ).<sup>60,61</sup> Moreover, the MLCT absorption transition energy difference of 1900  $\text{cm}^{-1}$  between  $\text{L} = \text{bpy}$  and **cpy** in  $[\text{ReCl}(\text{CO})_3\text{L}_2]$  in dichloromethane agreed well with the emission energy difference between **Re-bpy** and **Re-cpy**.<sup>61</sup> A similar trend was reported on the difference of the transition energy of the MLCT absorption band in  $[\text{Fe}(\text{CN})_5\text{L}]^{3-}$  ( $\text{L} = \text{bpy}$ , **pz**, **cpy**, or **4bzipy**) in  $\text{H}_2\text{O}$  (22800  $\text{cm}^{-1}$  for  $\text{L} = \text{bpy}$ , 21800  $\text{cm}^{-1}$  for  $\text{L} = \text{pz}$ , 21000  $\text{cm}^{-1}$  for  $\text{L} = \text{cpy}$ , and 20500  $\text{cm}^{-1}$  for  $\text{L} = 4\text{bzipy}$ ).<sup>62,63</sup> In the case of  $[\text{Cu}_2(\mu\text{-Br})_2(\text{PPh}_3)_2\text{L}_2]$  having an MLCT emissive excited state ( $\text{L} = 3\text{bzipy}$  or **4bzipy**), the emission energy difference of 2800  $\text{cm}^{-1}$  agreed with that between **Re-3bzipy** and **Re-4bzipy**.<sup>64</sup> Therefore, the degrees of emission-energy-shift values in the group B and **Re-3bzipy** complexes are very similar with those of the MLCT transition-energy-shift values observed in the complexes with the relevant ligand. To further discuss the excited-state characteristics of the group A and B and **Re-3bzipy** complexes, we calculated the radiative ( $k_r$ ) and nonradiative decay rate constants ( $k_{nr}$ ) on the basis of the relationship  $k_r = \Phi_{em}/\tau_{em}$  and  $\Phi_{em} = k_r/(k_r + k_{nr})$  in which weighted-averaged  $\tau_{em}$  values were adopted for complexes showing multiexponential emission decays. The  $k_{nr}$  and  $k_r$  values thus evaluated for each complex are included in Table 2. The  $k_{nr}$  values of the group A complexes at 296 K fall in the range of  $1.6 \times 10^3$ – $2.3 \times 10^4 \text{ s}^{-1}$ , while the relevant values of the group B and **Re-3bzipy** complexes vary significantly in the range of  $4.8 \times 10^4$ – $2.6 \times 10^7 \text{ s}^{-1}$ , demonstrating that the  $\Phi_{em}$  and  $\tau_{em}$  values of the group B complexes are governed by the nonradiative decay rate constant.<sup>65</sup> For the  $^3\text{MLCT}$  excited state represented by  $[\text{M}(\text{N}-\text{N})_3]^{2+}$  ( $\text{M} = \text{Ru}$ , **Os**;  $\text{N}-\text{N} = 2,2'$ -bipyridine derivatives or 1,10-phenanthroline derivatives), the emission energy ( $\nu_{em}$ ) of the complex is determined by the nature of a  $\text{N}-\text{N}$  ligand and, in such a case, the  $\nu_{em}$  value of the complex sometimes correlates linearly with the natural logarithm of the  $k_{nr}$  value: energy gap ( $\nu_{em}$ ) dependence of  $k_{nr}$ .<sup>66,67</sup> Because we suppose that the group B complexes possess the metal-to-N-heteroaromatic ligand charge-transfer excited triplet state, we plot the  $k_{nr}$  data of the complexes against the relevant  $\nu_{em}$  values. Figure 7 shows an energy gap ( $\nu_{em}$ ) dependence of  $\ln k_{nr}$  for the group A and B and **Re-3bzipy** complexes observed in the crystalline phase at 296 K. It is very clear that the data of the group B complexes and **Re-3bzipy** fall on a straight line, demonstrating that the nonradiative decay process is very similar among the group B complexes and **Re-3bzipy**. On the basis of these data, it is

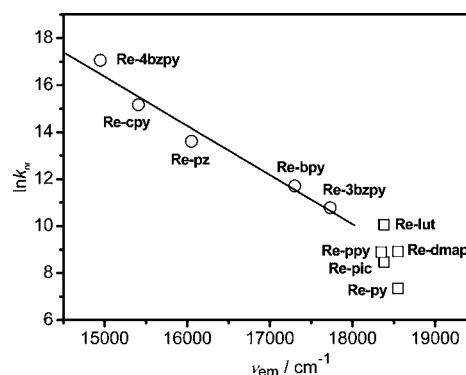


**Figure 7.** Plot of  $\ln k_{nr}$  against the emission maximum energy ( $\nu_{em}$ ) for the complexes in the group A (open squares) and group B (open circles) and **Re-3bzipy** (open circles) in the crystalline phase at 296 K.

suggested that the group B complexes exhibit  $^3\text{MLCT}$ -like emission. It is worth noting that the emission spectroscopic properties of **Re-3bzipy** at 296 and 77 K are very similar to those of the group B complexes; the longer-wavelength shift of  $\lambda_{em}$  compared with that of the group A complexes and no vibronic structure in the emission spectra at 77 K. On the other hand, the feature of the UV–vis reflectance spectrum is similar to those of the group A complexes. Therefore, it may be concluded that the emissive excited state is the inseparable mixture of  $^3\text{MLCT}$  and  $^3[(d_{xy})^1(d_{\pi^*})^1]$  excited states.

It should be noted that all of the technetium complexes showed  $\lambda_{em}$  values very similar to one another including the emission spectral band shapes with vibronic structures. These emission spectral patterns are very similar to those of the group A rhenium complexes. It is commonly recognized that the energy levels of the metal-centered orbitals in a technetium complex are stabilized compared with those in the rhenium analogues and the energy gap between the metal-centered HOMO and LUMO of a technetium complex is smaller than that of a rhenium analogue.<sup>68,69</sup> It is reasonable to assume that the  $d_{\pi^*}$  orbitals of **Tc-pz** and **Tc-cpy** are lower in energy, while those of **Re-pz** and **Re-cpy** are higher in energy than the  $\pi^*$  orbitals of **pz** and **cpy**, respectively. If an N-heteroaromatic ligand  $\pi^*$  orbital remains constant in energy, the LUMO of the technetium complex possesses metal character and that of the relevant rhenium complex has N-heteroaromatic ligand character. Therefore, the emissive excited states of **Tc-pz** and **Tc-cpy** are the metal-centered  $^3[(d_{xy})^1(d_{\pi^*})^1]$  states, and those of the isomorphous **Re-pz** and **Re-cpy** are best characterized by  $^3\text{MLCT}$  character.

## CONCLUSION

The tetracyanonitridorhenium(V) and -technetium(V) complexes with N-heteroaromatic ligands have been synthesized, and their spectroscopic and photophysical properties have been characterized. The pyridine coordinate rhenium(V) complex showed a quite high emission quantum yield: 0.93. In the present study, we demonstrated that the nature of the emissive excited state of the  $d^2$  nitridometal complex was controlled by the energy level of the N-heteroaromatic ligand to show  $^3[(d_{xy})^1(d_{\pi^*})^1]$  or a metal-to-N-heteroaromatic ligand charge-transfer ( $^3\text{MLCT}$ ) excited state. It is the first time that  $d^2$  oxo- or nitridometal complex exhibited the  $^3\text{MLCT}$ -type emission. The rhenium complexes exhibited two types of excited states by a change in the  $\pi^*$  level of the N-heteroaromatic ligand. All of the technetium complexes possessed a  $^3[(d_{xy})^1(d_{\pi^*})^1]$  excited

state because the electron occupied and unoccupied technetium-centered energy levels are lower than the  $\pi^*$  level of the N-heteroaromatic ligand.

## ■ ASSOCIATED CONTENT

### 📄 Supporting Information

Crystallographic data in CIF format, preparation procedures, tables of crystallographic data, and figures of IR and UV–vis reflectance spectra in the solid state. This material is available free of charge via the Internet at <http://pubs.acs.org>.

## ■ AUTHOR INFORMATION

### Corresponding Author

\*E-mail: [tyoshi@irrc.osaka-u.ac.jp](mailto:tyoshi@irrc.osaka-u.ac.jp). Tel: +81-6-6879-8821. Fax: +81-6-6879-8825.

### Notes

The authors declare no competing financial interest.

## ■ REFERENCES

- (1) Del Negro, A. S.; Wang, Z.; Seliskar, C. J.; Heineman, W. R.; Sullivan, B. P.; Hightower, S. E.; Hubler, T. L.; Bryan, S. A. *J. Am. Chem. Soc.* **2005**, *127*, 14978–14979.
- (2) Del Negro, A. S.; Seliskar, C. J.; Heineman, W. R.; Hightower, S. E.; Bryan, S. A.; Sullivan, B. P. *J. Am. Chem. Soc.* **2006**, *128*, 16494–16495.
- (3) Kurz, P.; Probst, B.; Spingler, B.; Alberto, R. *Eur. J. Inorg. Chem.* **2006**, 2966–2974.
- (4) Briggs, B. N.; McMillin, D. R.; Todorova, T. K.; Gagliardi, L.; Poineau, F.; Czerwinski, K. R.; Sattelberger, A. P. *Dalton Trans.* **2010**, 39, 11322–11324.
- (5) Chatterjee, S.; Del Negro, A. S.; Edwards, M. K.; Bryan, S. A.; Kaval, N.; Pantelic, N.; Morris, L. K.; Heineman, W. R.; Seliskar, C. J. *Anal. Chem.* **2011**, *83*, 1766–1772.
- (6) Chatterjee, S.; Del Negro, A. S.; Wang, Z.; Edwards, M. K.; Skomurski, F. N.; Hightower, S. E.; Krause, J. A.; Twamley, B.; Sullivan, B. P.; Reber, C.; Heineman, W. R.; Seliskar, C. J.; Bryan, S. A. *Inorg. Chem.* **2011**, *50*, 5815–5823.
- (7) Ikeda, H.; Yoshimura, T.; Ito, A.; Sakuda, E.; Kitamura, N.; Takayama, T.; Sekine, T.; Shinohara, A. *Inorg. Chem.* **2012**, *51*, 12065–12074.
- (8) Isovitsch, R. A.; Beadle, A. S.; Fronczek, F. R.; Maverick, A. W. *Inorg. Chem.* **1998**, *37*, 4258–4264.
- (9) Lanthier, E.; Bendix, J.; Reber, C. *Dalton Trans.* **2010**, 39, 3695–3705.
- (10) Winkler, J. R.; Gray, H. B. *J. Am. Chem. Soc.* **1983**, *105*, 1373–1374.
- (11) Winkler, J. R.; Gray, H. B. *Inorg. Chem.* **1985**, *24*, 346–355.
- (12) Newsham, M. D.; Giannelis, E. P.; Pinnavaia, T. J.; Nocera, D. G. *J. Am. Chem. Soc.* **1988**, *110*, 3885–3891.
- (13) Thorp, H. H.; Van Houten, J.; Gray, H. B. *Inorg. Chem.* **1989**, *28*, 889–892.
- (14) Neyhart, G. A.; Bakir, M.; Boaz, J.; Vining, W. J.; Sullivan, B. P. *Coord. Chem. Rev.* **1991**, *111*, 27–32.
- (15) Neyhart, G. A.; Seward, K. J.; Boaz, J.; Sullivan, B. P. *Inorg. Chem.* **1991**, *30*, 4486–4488.
- (16) Yam, V. W. W.; Tam, K. K.; Cheng, M. C.; Peng, S. M.; Wang, Y. J. *J. Chem. Soc., Dalton Trans.* **1992**, 1717–1723.
- (17) Yam, V. W. W.; Tam, K. K.; Lai, T. F. *J. Chem. Soc., Dalton Trans.* **1993**, 651–652.
- (18) Yam, V. W. W.; Tam, K. K. *J. Chem. Soc., Dalton Trans.* **1994**, 391–392.
- (19) Yam, V. W. W.; Tam, K. K.; Cheung, K. K. *J. Chem. Soc., Dalton Trans.* **1996**, 1125–1132.
- (20) Oetliker, U.; Savoie, C.; Stanislas, S.; Reber, C.; Connac, F.; Beauchamp, A. L.; Loiseau, F.; Dartiguenave, M. *Chem. Commun.* **1998**, 657–658.
- (21) Savoie, C.; Reber, C. *Coord. Chem. Rev.* **1998**, *171*, 387–398.
- (22) Savoie, C.; Reber, C. *J. Am. Chem. Soc.* **2000**, *122*, 844–852.
- (23) Yam, V. W. W.; Pui, Y. L.; Man-Chung Wong, K.; Cheung, K. K. *Inorg. Chim. Acta* **2000**, 300–302, 721–732.
- (24) Grey, J. K.; Triest, M.; Butler, I. S.; Reber, C. *J. Phys. Chem. A* **2001**, *105*, 6269–6272.
- (25) Bailey, S. E.; Eikey, R. A.; Abu-Omar, M. M.; Zink, J. I. *Inorg. Chem.* **2002**, *41*, 1755–1760.
- (26) Grey, J. K.; Butler, I. S.; Reber, C. *J. Am. Chem. Soc.* **2002**, *124*, 11699–11708.
- (27) Grey, J. K.; Marguerit, M.; Butler, I. S.; Reber, C. *Chem. Phys. Lett.* **2002**, *366*, 361–367.
- (28) Grey, J. K.; Butler, I. S.; Reber, C. *Can. J. Chem.* **2004**, *82*, 1083–1091.
- (29) Hopkins, M. D.; Miskowski, V. M.; Gray, H. B. *J. Am. Chem. Soc.* **1986**, *108*, 6908–6911.
- (30) Che, C.-M.; Yam, V. W. W.; Cho, K.-C.; Gray, H. B. *J. Chem. Soc., Chem. Commun.* **1987**, 948–949.
- (31) Sartori, C.; Preetz, W. *Z. Naturforsch., A: Phys. Sci.* **1988**, *43*, 239–247.
- (32) Che, C. M.; Lau, T. C.; Lam, H. W.; Poon, C. K. *J. Chem. Soc., Chem. Commun.* **1989**, 114–116.
- (33) Che, C.-M.; Lam, M. H.-W.; Mak, T. C. W. *J. Chem. Soc., Chem. Commun.* **1989**, 1529–1531.
- (34) Yam, V. W. W.; Che, C. M. *Coord. Chem. Rev.* **1990**, *97*, 93–104.
- (35) Yam, V. W. W.; Che, C.-M. *J. Chem. Soc., Dalton Trans.* **1990**, 3741–3746.
- (36) Lam, H.-W.; Chin, K.-F.; Che, C.-M.; Wang, R.-J.; Mak, T. C. W. *Inorg. Chim. Acta* **1993**, *204*, 133–137.
- (37) Che, C. M.; Wong, K. Y.; Lam, H. W.; Chin, K. F.; Zhou, Z. Y.; Mak, T. C. W. *J. Chem. Soc., Dalton Trans.* **1993**, 857–861.
- (38) Che, C.-M. *Pure Appl. Chem.* **1995**, *67*, 225–232.
- (39) Chin, K.-F.; Cheung, K.-K.; Yip, H.-K.; Mak, T. C. W.; Che, C. M. *J. Chem. Soc., Dalton Trans.* **1995**, 657–663.
- (40) Chin, K.-F.; Cheng, Y.-K.; Cheung, K.-K.; Guo, C.-X.; Che, C.-M. *J. Chem. Soc., Dalton Trans.* **1995**, 2967–2973.
- (41) Lai, S.-W.; Lau, T.-C.; Fung, W. K. M.; Zhu, N.; Che, C.-M. *Organometallics* **2003**, *22*, 315–320.
- (42) TEXSAN; Molecular Structure Corp.: The Woodlands, TX, 1985 and 1992.
- (43) *Crystal Structure*, version 4.0.1; Rigaku Corp.: Akishima, Japan, 2011.
- (44) Farrugia, L. J. *J. Appl. Crystallogr.* **1997**, *30*, 565.
- (45) Baldas, J.; Boas, J. F.; Colmanet, S. F.; Mackay, M. F. *Inorg. Chim. Acta* **1990**, *170*, 233–239.
- (46) Purcell, W.; Potgieter, I. M.; Damoense, L. J.; Leipoldt, J. G. *Transition Met. Chem.* **1992**, *17*, 387–389.
- (47) Britten, J. F.; Lock, C. J. L.; Wei, Y. *Acta Crystallogr., Sect. C* **1993**, *C49*, 1277–1280.
- (48) Yoshimura, T.; Umakoshi, K.; Sasaki, Y.; Ishizaka, S.; Kim, H.-B.; Kitamura, N. *Inorg. Chem.* **2000**, *39*, 1765–1772.
- (49) Bendix, J.; Meyer, K.; Weyhermueller, T.; Bill, E.; Metzler-Nolte, N.; Wieghardt, K. *Inorg. Chem.* **1998**, *37*, 1767–1775.
- (50) Bendix, J.; Deeth, R. J.; Weyhermüller, T.; Bill, E.; Wieghardt, K. *Inorg. Chem.* **2000**, *39*, 930–938.
- (51) Abram, U.; Spies, H.; Görner, W.; Kirmse, R.; Stach, J. *Inorg. Chim. Acta* **1985**, *109*, L9–L11.
- (52) Baldas, J.; Bonnyman, J.; Williams, G. A. *Inorg. Chem.* **1986**, *25*, 150–153.
- (53) Baldas, J.; Bonnyman, J. *Inorg. Chim. Acta* **1988**, *141*, 153–154.
- (54) De Vries, N.; Costello, C. E.; Jones, A. G.; Davison, A. *Inorg. Chem.* **1990**, *29*, 1348–1352.
- (55) Cros, G.; Belhadj Tahar, H.; de Montauzon, H.; Gleizes, A.; Coulais, Y.; Guiraud, R.; Bellande, E.; Pasqualini, R. *Inorg. Chim. Acta* **1994**, *227*, 25–31.
- (56) Bolzati, C.; Boschi, A.; Uccelli, L.; Tisato, F.; Refosco, F.; Cagnolini, A.; Duatti, A.; Prakash, S.; Bandoli, G.; Vittadini, A. *J. Am. Chem. Soc.* **2002**, *124*, 11468–11479.



- (57) Bolzati, C.; Cavazza-Ceccato, M.; Agostini, S.; Tisato, F.; Bandoli, G. *Inorg. Chem.* **2008**, *47*, 11972–11983.
- (58) Schroer, J.; Abram, U. *Polyhedron* **2011**, *30*, 2157–2161.
- (59) Juris, A.; Balzani, V.; Barigelletti, F.; Campagna, S.; Belser, P.; Von Zelewsky, A. *Coord. Chem. Rev.* **1988**, *84*, 85–277.
- (60) Giordano, P. J.; Fredericks, S. M.; Wrighton, M. S.; Morse, D. L. *J. Am. Chem. Soc.* **1978**, *100*, 2257–2259.
- (61) Giordano, P. J.; Wrighton, M. S. *J. Am. Chem. Soc.* **1979**, *101*, 2888–2897.
- (62) Alshehri, S.; Burgess, J.; Morgan, G. H.; Patel, B.; Patel, M. S. *Transition Met. Chem* **1993**, *18*, 619–622.
- (63) Lavalley, D. K.; Baughman, M. D.; Phillips, M. P. *J. Am. Chem. Soc.* **1977**, *99*, 718–724.
- (64) Araki, H.; Tsuge, K.; Sasaki, Y.; Ishizaka, S.; Kitamura, N. *Inorg. Chem.* **2005**, *44*, 9667–9675.
- (65) The  $k_{nr}$  value of **Re-4bzipy** is calculated from the approximate expression  $k_{nr} = 1/\tau_{em}$ , which is adopted for the small  $\Phi_{em}$  value.
- (66) Caspar, J. V.; Kober, E. M.; Sullivan, B. P.; Meyer, T. J. *J. Am. Chem. Soc.* **1982**, *104*, 630–632.
- (67) Caspar, J. V.; Meyer, T. J. *J. Am. Chem. Soc.* **1983**, *105*, 5583–5590.
- (68) Yoshimura, T.; Ikai, T.; Tooyama, Y.; Takayama, T.; Sekine, T.; Kino, Y.; Kirishima, A.; Sato, N.; Mitsugashira, T.; Takahashi, N.; Shinohara, A. *Eur. J. Inorg. Chem.* **2010**, 1214–1219.
- (69) Yoshimura, T.; Ikai, T.; Takayama, T.; Sekine, T.; Kino, Y.; Shinohara, A. *Inorg. Chem.* **2010**, *49*, 5876–5882.